Novel regularization scheme for nucleon-nucleon lattice simulations with effective field theory

M. Ahmadi*

Department of Physics, University of Tehran, PO Box 14395-547, Tehran, Iran

M. R. Hadizadeh of

College of Engineering, Science, Technology and Agriculture, Central State University, Wilberforce, Ohio 45384, USA and Department of Physics and Astronomy, Ohio University, Athens, Ohio 45701, USA

M. Radin •

Department of Physics, K. N. Toosi University of Technology, PO Box 16315-1618 Tehran, Iran

S. Bayegan[§]

Department of Physics, University of Tehran, PO Box 14395-547, Tehran, Iran

(Received 26 May 2020; accepted 25 September 2020; published 14 October 2020)

We propose a new regularization scheme to study the bound state of two-nucleon systems in lattice effective field theory. Inspired by a continuum effective field theory calculation, we study an exponential regulator acting on the leading-order and next-to-leading order interactions, consisting of local contact terms. By fitting the low-energy coefficients to deuteron binding energy and the asymptotic normalization coefficient on a lattice simulation, we extract the effective range expansion (ERE) parameters in the 3S_1 channel to order p^2 . We explore the impact of different powers of the regulator on the extracted ERE parameters for the lattice spacing a = 1.97 fm. Moreover, we investigate how the implementation of the regularization scheme improves the predicted ERE parameters on the lattice spacing in the range of $1.4 \le a \le 2.6$ fm. Our numerical analysis indicates that for lattice spacing greater than 2 fm, the predicted observables are very close to the experimental data.

DOI: 10.1103/PhysRevC.102.044001

I. INTRODUCTION

Nuclear lattice effective field theory (NLEFT) is a modelindependent and precision controlled approach for the calculation of bound and scattering state properties in nuclear physics [1]. The novel combination of lattice methods with an effective field theory approach has been pursued successfully for few- and many-body systems.

The first attempts for an exact solution of infinite nuclear matter using Monte Carlo methods are performed in Ref. [2], indicating that energy and saturation properties of symmetric nuclear matter can be reproduced from lattice simulations. The *ab initio* techniques combine the Monte Carlo methods with the low-energy EFT, known as chiral effective field theory. Based on these approaches, our information for the scattering of light nuclei, and the ground-state properties of light-, medium-mass nuclei, as well as neutron matter has been compromised [3–8]. To improve the efficiency of large-scale calculations of nucleus-nucleus scattering and reactions using Monte Carlo calculations, the adiabatic projection method is developed on lattice [9,10]. The accuracy

and efficiency of the method are tested on fermion-dimer scattering calculations in lattice EFT.

The bound state of two nucleons on a lattice, mainly in the S-wave channel, is formulated in pionless EFT at the next to leading order (NLO) [11]. The lattice spacing dependence of the renormalization group flows is studied while the deuteron binding energy and the asymptotic normalization coefficient (ANC) are being fixed. Lüscher has shown how one can connect the quantities obtained on a finite volume to the infinite volume physical observables by connecting the box size dependence of energy eigenvalues on a lattice to the effective range parameter and the scattering length [12]. The exact solution of Lüscher formula for the energy levels of the two-nucleon system on a lattice with periodic boundary conditions for the extraction of scattering parameters has been implemented by Beane et al. in a pionless EFT approach [13]. They have shown that lattice simulations with $L \ge 15$ fm will provide information on the scattering lengths and effective ranges straightforwardly. Whereas the extraction of data from lattice simulations with $L \leq 10 \,\mathrm{fm}$ requires direct matching to $p \cot \delta_0(p)$ in the spin-singlet channel and considering the mixing between the S and D waves remains challenging. The impact of the topological finite-volume corrections in lattice calculations of three-nucleon bound state [14], the elastic scattering of fermion-dimer [15], and also neutron-deuteron scattering at the very low energies [16] are studied in a pionless EFT approach.

^{*}masoumehahmadi@ut.ac.ir

[†]mhadizadeh@centralstate.edu

[‡]radin@kntu.ac.ir

[§]Corresponding author: bayegan@ut.ac.ir

One of the main challenges of lattice calculations is the necessity to eliminate errors caused by the nonvanishing lattice spacing. One approach to eliminate the lattice artifacts is including the irrelevant higher-dimensional operators into the lattice action, which leads to faster convergence to the continuum limit [17]. Since the lattice spacing serves as a natural ultraviolet (UV) regulator for the theory, another practical strategy is the application of a regulator to utilize the smearing of the contact interactions. Klein et al. have shown that the application of different regularization schemes leads to the lattice spacing independence of observables for a wide range of the lattice spacing in the range $0.5 \le a \le 2.0$ fm [18]. This study is performed at the leading order of pionless and pionful EFT. The extension of the calculations to the two-, three-, and four-body sectors to study the lattice spacing dependence up to next-to-next-to-leading order (N²LO), including twoand three-nucleon interactions, is performed in Ref. [19]. The binding energy correlation of triton and helium-4 is studied for various lattice spacings $a = 1.97, 1.64, 1.32 \,\mathrm{fm}$, and it is shown how the convergence towards the Tjon line is reached for smaller lattice spacing. A systematic study of neutronproton scattering, in terms of the computationally efficient radial Hamiltonian method, is studied on a lattice EFT up to N²LO [20]. A regularization scheme is applied only to the LO contact interactions. The lattice spacing dependence of the scattering observables is explored for lattice spacings ranging from a = 1.97 fm down to a = 0.98 fm, and it is shown at a = 0.98 fm, the lattice artifacts appear to be small. In a recent study by Eliyahu et al., the effect of the finite lattice size on the binding energies of light nuclei is explored by the construction of pionless EFT at the LO, where a gaussian regulator is applied on the contact terms [21].

In this paper, we propose a regularization scheme, inspired by continuum EFT calculations, to study the two-nucleon systems on a lattice and extract the effective range expansion (ERE) parameters for a wide range of lattice spacing. In Sec. II, we briefly review the formalism of two-nucleon bound state on a lattice, projected in the ${}^{3}S_{1}$ channel, using pionless EFT up to NLO. By introducing the Lagrangian and Hamiltonian of the two-nucleon system on a lattice, the explicit form of the Lippmann-Schwinger equation is presented by considering the contact interactions between nucleons. In Sec. III, the procedure of extraction of physical ERE parameters from finite volume energy eigenvalues is discussed. Our numerical results for the lattice energy eigenvalues obtained for different lattice spacing parameters and different numbers of lattice nodes are presented in Sec. IV. Moreover, a new regularization scheme is introduced, and the impact of the regularization scheme on the ERE parameters is studied in detail. A conclusion is provided in Sec. V. All the energy eigenvalues obtained for different lattice spacing parameters are provided in the Appendix.

II. TWO-NUCLEON IN 3S_1 CHANNEL IN PIONLESS LATTICE EFT UP TO NLO

At very low energies where the nucleon momentum is much smaller than the pion mass, i.e., $Q \ll m_{\pi}$, few-nucleon systems are not sensitive to the details of the nucleon-nucleon

interactions. So, an EFT is constructed by low energy degrees of freedom and the Lagrangian is formulated as all contact interactions between nucleons that are allowed by symmetry. In this section, we consider the NLO Lagrangian of pionless EFT. The nucleon-nucleon interactions are defined by an infinite number of local operators with an increasing number of derivatives acting on the nucleon fields. The isospin SU(2) symmetric and nonrelativistic Lagrangian in the continuum is given by

$$\mathcal{L} = N^{\dagger} \left[i \partial_t + \frac{\nabla^2}{2M} \right] N - C_0 (N^T P^k N)^{\dagger} (N^T P^k N)$$
$$+ C_2 \left[(N^T P^k N)^{\dagger} (N^T P^k \overrightarrow{\nabla}^2 N) + \text{H.c.} \right], \tag{1}$$

where N denotes the nonrelativistic nucleon field, M is nucleon mass, the low-energy constants (LECs) C_0 and C_2 are the zero-range interaction strengths, and $\overrightarrow{\nabla}^2 = \overleftarrow{\nabla} \overleftarrow{\nabla} - 2\overleftarrow{\nabla} \overrightarrow{\nabla} + \overrightarrow{\nabla} \overrightarrow{\nabla}$. $P^k = \frac{1}{\sqrt{8}}\sigma_2\sigma^k\tau_2$, with the vector indices k = 1, 2, 3, is the projection operator for 3S_1 channel, where σ_2 and τ_2 are the Pauli matrices acting on the spin and isospin spaces, respectively. The Hamiltonian corresponding to the Lagrangian of Eq. (1) is given by

$$H = \int d^3x \left[N^{\dagger} \left(\frac{-\nabla^2}{2M} \right) N + C_0 (N^T P^k N)^{\dagger} (N^T P^k N) - C_2 ((N^T P^k N)^{\dagger} (N^T P^k \overrightarrow{\nabla}^2 N) + \text{H.c.}) \right].$$
 (2)

To study the bound state of two-nucleon systems on a lattice, we utilize a cubic box of side length L with periodic boundary conditions. The lattice spacing between lattice nodes is a, so that $L = N_s a$, where N_s is the number of nodes in each spatial direction. As it is shown in Ref. [11], in order to transform the Hamiltonian of Eq. (2) from the continuum to a dimensionless Hamiltonian on a lattice, one needs to apply the following substitutions:

$$N(\mathbf{x}) \to N_{\mathbf{n}} a^{-3/2}, \quad \mathbf{x} \to \mathbf{n} a, \quad \int d^3 x \to a^3 \sum_{\mathbf{n}},$$
 $H \to H_L a^{-1}, \quad M \to M_L a^{-1},$
 $C_0 \to C_0^L a^2, \quad C_2 \to C_2^L a^4,$ (3)

where $\mathbf{n} = (n_1, n_2, n_3)$ is a three-dimensional vector with integer components and C_0^L , C_2^L , and M_L are dimensionless parameters, corresponding to parameters C_0 , C_2 , and M in continuum. The lattice Hamiltonian H_L can be obtained in terms of dimensionless quantities as

$$H_{L} = \sum_{\mathbf{n}} \left[\frac{-1}{2M_{L}} N_{\mathbf{n}}^{\dagger} \nabla_{L}^{2} N_{\mathbf{n}} + C_{0}^{L} (N_{\mathbf{n}}^{T} P^{k} N_{\mathbf{n}})^{\dagger} (N_{\mathbf{n}}^{T} P^{k} N_{\mathbf{n}}) - C_{2}^{L} \left\{ (N_{\mathbf{n}}^{T} P^{k} N_{\mathbf{n}})^{\dagger} (N_{\mathbf{n}}^{T} P^{k} \overrightarrow{\nabla}_{L}^{2} N_{\mathbf{n}}) + \text{H.c.} \right\} \right],$$
(4)

where ∇_L^2 and $\overrightarrow{\nabla}_L^2$ represent the discretization of the dimensionless Laplacian. By considering the nucleon operator N_n in

TABLE I. Hopping coefficients ω_i for different levels of improvement up to $\mathcal{O}(a^4)$ in the free nucleon lattice action [6].

	Unimproved	$\mathcal{O}(a^2)$ improved	$\mathcal{O}(a^4)$ improved
ω	1	5/4	49/36
ω_1	1	4/3	3/2
ω_2	0	1/12	3/20
ω_3	0	0	1/90

momentum space as

$$N_{\mathbf{n}} = \frac{1}{N_s^{3/2}} \sum_{\mathbf{p}_L} e^{i\mathbf{p}_L \cdot \mathbf{n}} a_{\mathbf{p}_L}, \tag{5}$$

the lattice Hamiltonian of Eq. (4) leads to

$$H_{L} = \sum_{\mathbf{p}_{L}} \frac{\mathcal{P}_{L}}{2M_{L}} a_{\mathbf{p}_{L}}^{\dagger} a_{\mathbf{p}_{L}} + \frac{1}{N_{s}^{3}} \sum_{\mathbf{p}_{L}, \mathbf{p}_{L}'} \left(C_{0}^{L} + 4C_{2}^{L} (\mathcal{P}_{L} + \mathcal{P}_{L}') \right)$$

$$\times \left(a_{\mathbf{p}_{L}}^{\dagger} P^{k} a_{-\mathbf{p}_{L}}^{\dagger} \right) \left(a_{\mathbf{p}_{L}^{\prime}} P^{k} a_{-\mathbf{p}_{L}^{\prime}} \right). \tag{6}$$

The momentum argument \mathcal{P}_L obtained from the free nucleon lattice action, improvement up to $\mathcal{O}(a^4)$, defined as [6]

$$\mathcal{P}_L \equiv 2\sum_{i=1}^3 (\omega - \omega_1 \cos(p_i) + \omega_2 \cos(2p_i) - \omega_3 \cos(3p_i)), \tag{7}$$

where the components of the lattice momentum $\mathbf{p}_L \equiv (p_1, p_2, p_3)$ under the periodic boundary condition takes the values

$$p_i = \frac{2\pi}{N_s} \hat{p}_i, \quad -\frac{N_s}{2} < \hat{p}_i \leqslant \frac{N_s}{2}, \quad i = 1, 2, 3.$$
 (8)

As it is shown in Ref. [6], the hopping coefficients ω_i in the improved free nucleon action eliminate lattice artifacts in the Taylor expansion of single-nucleon dispersion relation around $\mathbf{p}_L = 0$ up to the indicated order. The coefficients ω_i for different level of improvement up to $\mathcal{O}(a^4)$, are listed in Table I. It should be noticed that the $\mathcal{O}(a^{2n})$ -improved lattice action corresponds to a lattice derivative which contains 2n+2 nearest neighbors, or a total of 2n+3 lattice sites. It means unimproved, $\mathcal{O}(a^2)$ -improved, and $\mathcal{O}(a^4)$ -improved actions are corresponding to three-, five-, and seven-point

formula, respectively. By considering the lattice Hamiltonian of Eq. (6), the lattice form of Lippmann-Schwinger equation for two-nucleon bound state can be obtained as [11]

$$\psi(\mathbf{p}_L) = \frac{1}{E_L - \frac{\mathcal{P}_L}{M_L}} \frac{1}{N_s^3} \sum_{\mathbf{p}_L'} \left(C_0^L + 4C_2^L(\mathcal{P}_L + \mathcal{P}_L') \right) \psi(\mathbf{p}_L'), \tag{9}$$

where $E_L = Ea$ is the dimensionless two-nucleon binding energy and $\psi(\mathbf{p}_L)$ is the discretized two-nucleon wave function.

III. EXTRACTION OF EFFECTIVE RANGE EXPANSION PARAMETERS IN LATTICE

By solving the discretized form of the Lippmann-Schwinger equation of Eq. (9), one can obtain the two-nucleon energy eigenvalues on the lattice. In the following, we briefly show how the Lüscher formula can be used to extract the ERE parameters in 3S_1 channel by having the deuteron binding energy spectrum on the lattice. Lüscher has shown how one can connect the physical quantities in a finite volume to the real physics by connecting the box size dependence of the energy eigenvalues in a finite volume to the infinite volume scattering matrix. As it is shown in Ref. [13], the low-momentum behavior of the *S*-wave phase shift δ_0 , for two nucleons with a relative momentum p, can be described by the following ERE:

$$p \cot \delta_0(p) = -\frac{1}{a^{({}^3S_1)}} + \frac{1}{2}r^{({}^3S_1)} p^2 + \dots$$
$$= \frac{1}{\pi L}S(\eta), \tag{10}$$

where $a^{({}^{3}S_{1})}$ and $r^{({}^{3}S_{1})}$ refer to the scattering length and the effective range, respectively. $S(\eta)$ is the three-dimensional zeta function with the dimensionless argument $\eta = \left(\frac{Lp}{2\pi}\right)^{2}$. For $|\eta| < 1$, $S(\eta)$ can be expanded in powers of η as

$$S(\eta) = -\frac{1}{\eta} + S_0 + S_1 \eta + S_2 \eta^2 + S_3 \eta^3 + \dots,$$
 (11)

where the first few coefficients S_i are given as

$$S_0 = -8.913631$$
, $S_1 = 16.532288$, $S_2 = 8.401924$, $S_3 = 6.945808$,

TABLE II. The LECs C_0^L and C_2^L obtained at LO and NLO for different levels of improvement in the lattice momentum \mathcal{P}_L , defined in Eq. (7), to reproduce deuteron binding energy $E_d = -2.224575$ MeV and ANC = 0.249424 fm^{-0.5} for the lattice parameter a = 1.97 fm and $N_s = 20$.

Improvement Level	C_0^L	$C_2^L \times 10^{-2}$	E_2 (MeV)	ANC $(fm^{-0.5})$
		LO	1	
Unimproved	-0.49656112	0	-2.224575	0.186319
$\mathcal{O}(a^2)$ improved	-0.5792460	0	-2.224574	0.200483
$\mathcal{O}(a^4)$ improved	-0.60920561	0	-2.224575	0.204060
		NLO)	
Unimproved	-1.49576	+3.711484	-2.224574	0.249423
$\mathcal{O}(a^2)$ improved	-1.56064	+3.173400	-2.224575	0.249425
$\mathcal{O}(a^4)$ improved	-1.57907	+3.0453214	-2.224575	0.249425

$$S_4 = 6.426119, \quad S_5 = 6.202149,$$

 $S_6 = 6.098184, \quad S_7 = 6.048263.$ (12)

By considering the connection between the two-nucleon energy levels $E_2 = E_L/a = \frac{p^2}{M}$ and the argument η , i.e., $E_L = \frac{\eta a}{M}(\frac{2\pi}{L})^2$, one can obtain a set of η for a set of energy eigenvalues E_L obtained for a given lattice parameter a and different values of N_s or the box side length L. By using Eq. (11), the function $\frac{1}{\pi L}S(\eta)$ can be obtained for different values of η dictated by energy eigenvalues E_L . Finally by using a linear fitting to Eq. (10), one can extract the ERE parameters $a^{(3S_1)}$ and $r^{(3S_1)}$.

IV. NUMERICAL RESULTS

A. LECs and different levels of improvement in the lattice momentum argument \mathcal{P}_L

In this section, we study the effect of different levels of improvement, up to $\mathcal{O}(a^4)$, in the lattice momentum defined in Eq. (7) to solve the lattice form of Lippmann-Schwinger Eq. (9). To this aim, we solve the discretized Lippmann-Schwinger equation for the lattice spacing a = 1.97 fm with the number of nodes $N_s = 20$. The equation can be solved with both direct and Lanczos methods. Our numerical analysis shows that the runtime of the calculations with the direct approach increases exponentially with the number of nodes N_s . For instance, a direct diagonalization of the kernel of Eq. (9) for $N_s = 20$ takes about 90 minutes, while an iterative solution with the Lanczos technique (see Appendix C2 of Ref. [22]) takes about 1 s, both performed on a single-node CPU desktop. While we are convinced that both methods yield the same results for lattice deuteron binding energy and wave function, we perform all the calculations with the Lanczos technique to save runtime. Equation (9) is an eigenvalue equation in the form of $\lambda \psi = \mathcal{K}(E_L)\psi$ with the eigenvalue $\lambda = 1$. Since the kernel of the equation $\mathcal{K}(E_L)$ is energy dependent, the solution of the eigenvalue Eq. (9) can be started by an initial guess for the energy E_L and the search in the binding energy is stopped when $|1 - \lambda| \le 10^{-6}$.

The LEC C_0^L at LO is fitted to deuteron binding energy $E_d=-2.224575$ MeV, while at NLO, both LECs C_0^L and C_2^L are determined simultaneously by fitting to deuteron binding energy as well as the asymptotic normalization coefficient ANC = 0.249424 fm $^{-0.5}$. The value of ANC is extracted from the expression for the *S*-wave asymptotic normalization coefficient ANC = $\frac{1}{\sqrt{4\pi}}\sqrt{\frac{2k_0}{1-r^{(3S_1)}k_0}}$ [23], with $k_0=\sqrt{M|E_d|}$ and the experimental value of $r^{(3S_1)}=1.759(5)$ fm. Similar to the procedure performed in Ref. [11], the ANC parameter can been extracted by fitting the numerical lattice deuteron wave function $\psi(\mathbf{p}_L)$ to the analytical wave function $\psi(\mathbf{p}_L)=A+\frac{B}{M_L|E_L|+\mathcal{P}_L}$, with ANC = $\frac{B}{4\pi}$. To extract the physical values of LECs C_0^L and C_2^L . Eq. (9) is solved for a wide range of coefficients C_0^L and C_2^L . In Table II, we have listed the obtained

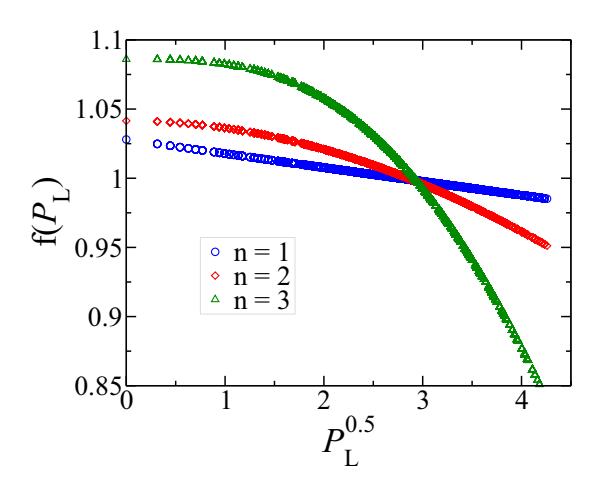


FIG. 1. The functional form of the regulator $f(\mathcal{P}_L)$, defined in Eq. (14), for n = 1 (the blue circles), n = 2 (the red diamonds), and n = 3 (the green triangles) with the regulator parameter b = 0.01.

LECs at LO and NLO for different levels of improvement. As we can see at LO, the improvements up to $\mathcal{O}(a^2)$ and $\mathcal{O}(a^4)$ lead to about 17% and 23% increasing in the absolute value of C_0^L , respectively. While at NLO, the improvements up to $\mathcal{O}(a^2)$ and $\mathcal{O}(a^4)$ lead to about 4% (14%) and 6% (18%) increasing (decreasing) in the absolute value of C_0^L (C_2^L), respectively. In order to minimize the lattice artifacts in our numerical study, for the rest of the paper we use $\mathcal{O}(a^4)$ improvement in the lattice momentum \mathcal{P}_L .

B. A new regularization scheme in lattice

In this section, we introduce a new regularization scheme and study its impact on the ERE parameters $a^{({}^3S_1)}$ and $r^{({}^3S_1)}$ obtained from the lattice energy eigenvalues E_L for different values of lattice spacing. Inspired by continuum EFT calculations [24], we consider the exponential regulators in the lattice nucleon-nucleon interactions $V_{NN}^L(\mathcal{P}_L, \mathcal{P}_L')$ as

$$V_{NN}^{L}(\mathcal{P}_L, \mathcal{P}_L') \to V_{NN}^{L}(\mathcal{P}_L, \mathcal{P}_L') f(\mathcal{P}_L) f(\mathcal{P}_L'),$$
 (13)

where the regulators are defined as

$$f(\mathcal{P}_L) = \frac{1}{f_0} \exp\left(-b\mathcal{P}_L^{n/2}/n\right); \ f_0 = \frac{1}{N_s^3} \sum_{\mathbf{p}_L} \exp\left(-b\mathcal{P}_L^{n/2}/n\right).$$
(14)

It should be noticed that the $\mathcal{P}_L^{n/2}$ is calculated from the lattice momentum argument \mathcal{P}_L , defined in Eq. (7). The regulator parameter b is dependent on the lattice spacing parameter a and is defined as $ba^3 = \mathcal{A}$. A typical value of the regularization parameter in our calculations for the lattice spacing $a=1.97\,\mathrm{fm}$ is b=0.01, which leads to the constant parameter $\mathcal{A}=7.645373\times 10^{-2}\,\mathrm{fm}^3$. In Fig. 1, we have shown the regulator $f(\mathcal{P}_L)$ as a function of the lattice momentum $\mathcal{P}_L^{0.5}$ for three exponential powers n=1,2,3 with the regulator parameter b=0.01. The lattice momentum argument \mathcal{P}_L is obtained for $N_s=20$. To study the effect of the regulators on the prediction of the ERE parameters $a^{(3S_1)}$ and $r^{(3S_1)}$, we solve Eq. (9) with different regulator powers for the lattice spacing $a=1.97\,\mathrm{fm}$ and $N_s=20$. For each power of the regulator,

 $^{^{1}}$ The factor $\frac{1}{\sqrt{4\pi}}$ comes from the normalization of the spherical harmonics.

TABLE III. Deuteron binding energy, ANC, and the ERE parameters $a^{(^3S_1)}$ and $r^{(^3S_1)}$ calculated for the lattice spacing parameter a = 1.97 fm. n, b indicates the parameters of the regulator, defined in Eq. (14). The numbers in parentheses are the uncertainties in the last digits.

Order	n, b	C_0^L	$C_2^L \times 10^{-2}$	E_2 (MeV)	ANC (fm ^{-0.5})	$a^{(^3S_1)}$ (fm)	$r^{(^3S_1)}$ (fm)
LO	1, 0	-0.60920561	0	-2.224575	0.204060	4.577(7)	0.496(8)
LO	1, 0.01	-0.6017484	0	-2.224573	0.199551	4.652(7)	0.621(7)
LO	2, 0.01	-0.5929415	0	-2.224576	0.195223	4.624(7)	0.580(8)
LO	3, 0.01	-0.569575	0	-2.224575	0.184159	4.64(1)	0.60(1)
NLO	1, 0	-1.57907	+3.0453214	-2.224575	0.249425	5.35(3)	1.65(2)
NLO	1, 0.01	-1.59677	+3.2940765	-2.224575	0.249424	5.43(5)	1.74(4)
NLO	2, 0.01	-1.587607	+3.4237993	-2.224574	0.249423	5.41(4)	1.73(3)
NLO	3, 0.01	-1.574284	+3.945544	-2.224575	0.249427	5.42(3)	1.76(2)
Experiment	_	_	_	-2.224575	0.249424	5.424(4)	1.759(5)

we refit the LECs in such a way that C_0^L and C_2^L reproduce the deuteron binding energy and the ANC. Then by having the LECs, we resolve Eq. (9) to calculate the energy eigenvalues E_L for smaller values of N_s , in the domain $4 \le N_s \le 20$. Finally, by applying the Lüscher formula, as discussed in Sec. III, we extract the ERE parameters from the energy eigenvalues. We implement the same steps at the LO, where the only LEC parameter C_0^L reproduces the deuteron binding energy, and we have no control over the ANC. In Table III, we have presented our numerical results for the prediction of the ERE parameters $a^{(^3S_1)}$ and $r^{(^3S_1)}$, with different powers of the regulator. At the NLO, deuteron binding energy and ANC are both used as inputs to extract the LECs C_0^L and C_2^L , while at the LO, the only input to extract C_0^L is deuteron binding energy. As we can see, applying the regulator leads to a correction in the ERE parameters, and it seems the power n = 1 leads to more corrections than n = 2 and n = 3.

In Fig. 2, we have shown the effective range function, in the 3S_1 neutron-proton channel, calculated for lattice spacing $a=1.97\,\mathrm{fm}$ as a function of the square of relative momentum. The results are shown at the LO and NLO. As we have discussed earlier, by using a linear fit to our data and matching to Eq. (10), one can extract the infinite volume ERE parameters from the finite volume energy eigenvalues. The impact of different power of regulators (for n=1,2,3) on

our data for the effective range function is shown. As we can see, all regulators, independent of their power, are increasing the slope and decreasing the absolute value of the vertical intercept of the effective range function, indicating an increase in the scattering length and effective range parameter. In the following, we discuss the impact of the regulator function on the ERE parameters extracted from different lattice spacing. In the first step, we have calculated the lattice energy eigenvalues with and without the regularized interactions for different lattice spacing values. To this aim, we have considered a regulator with a power one. Starting with $N_s = 20$, we extract the LECs C_0^L and C_2^L for different lattice spacing parameters $a=1.4,\,1.7,\,1.97,\,2.3,\,2.6$ fm, by fitting to the physical deuteron binding energy and ANC. This procedure leads to negative C_0^L and positive C_2^L for all considered lattice spacing parameters. Then by having the physical LECs, we have obtained a spectrum of the energy eigenvalues by lowering the number of nodes to $N_s = 4$. Finally, by using Lüscher formula in Eq. (10), we extract the ERE parameters. In Fig. 3, our numerical results for deuteron binding energies obtained from the solution of Eq. (9), are shown as a function of the number of lattice nodes N_s , with and without using the regularized interactions. All the calculated energy eigenvalues used in Fig. 3 are given in the Appendix. The obtained effective range functions with different lattice

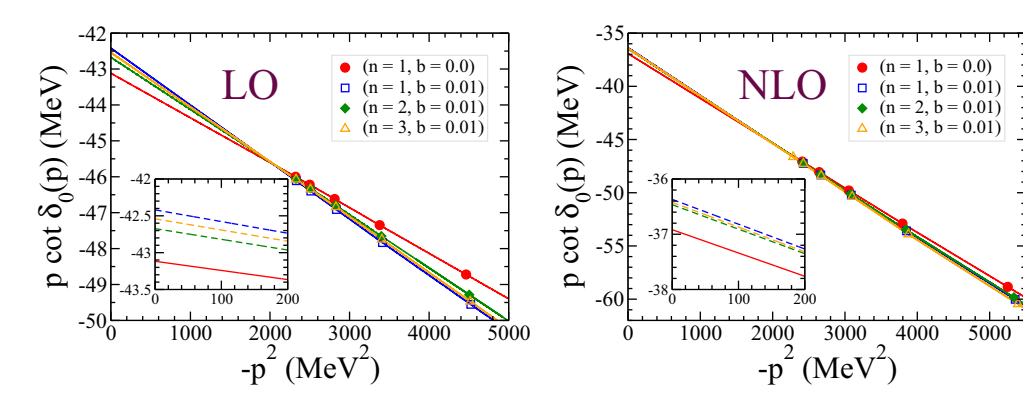


FIG. 2. The LO (left panel) and NLO (right panel) EFT results for the effective range function $p \cot \delta_0(p)$ in the 3S_1 neutron-proton channel for the lattice spacing a=1.97 fm, with and without regulators. The solid red line (circles) indicates the results obtained by bare contact interactions with no regulator. The blue (squares), green (diamonds), and orange (triangles) dashed lines are corresponding to the results obtained with regularized interactions with a regulator power n=1,2, and 3, respectively.

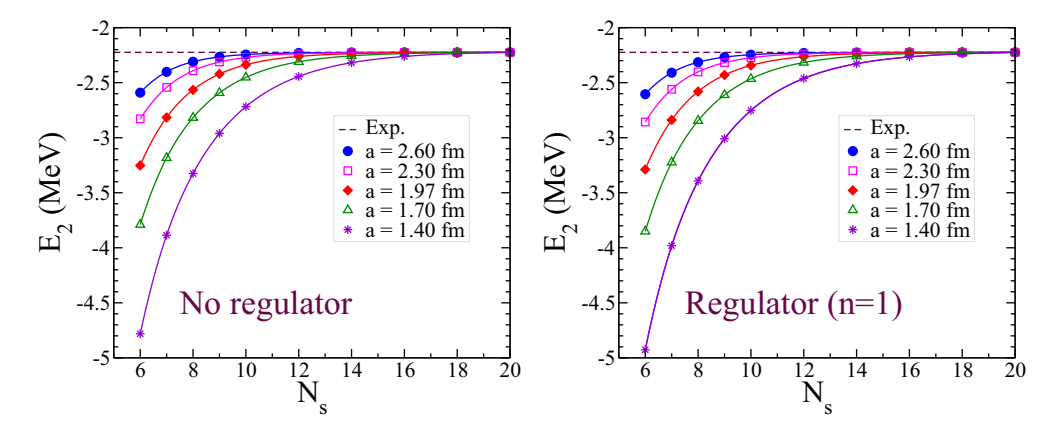


FIG. 3. The NLO EFT results for deuteron binding energy as a function of the number of lattice nodes N_s for different lattice spacing parameters a. In the left panel, the results are obtained with bare contact interactions with no regulator, and in the right panel, a regulator with power n = 1 and the parameter b = 0.01 is applied.

spacing $a = 1.4, 1.7, 1.97, 2.3, 2.6 \,\text{fm}$ are shown in Fig. 4. Our numerical results for extracted ERE parameters, with and without applying the regularization scheme, are presented in Table IV. It should be noticed that the LECs C_0^L and C_2^L are fitted to the experimental values of deuteron binding energy and ANC with $N_s = 20$. As we can see, the regularization scheme for lattice spacing greater than 2 fm, brings the scattering length parameters $a^{(^3S_1)}$ very close to the experimental value. Similarly, the regularization scheme increases the effective ranges $r^{(3S_1)}$ to values closer to the corresponding experimental value. So, we are confident that the introduced regularization scheme improves the extracted ERE parameters for different lattice spacing at NLO pionless EFT. It should be mentioned that we have not manipulated the regularization parameter b to reach the same ERE parameters for different lattice spacing. As it is shown earlier, the regulator parameter b is dependent on the lattice spacing a as $b = A/a^3$, while the value of A is considered to be constant for all lattice spacing. While the regularization scheme for smaller lattice spacing does not match the ERE parameters precisely to the corresponding experimental data, it brings them closer to the experimental data.

In Table V, we have compared our ERE parameters extracted for lattice spacing a = 1.97 fm, by different powers of the regulator, with the results of other studies.

V. CONCLUSION

In this paper, we have studied the impact of a new regularization scheme on the extraction of the ERE parameters of ${}^{3}S_{1}$ channel for different lattice spacing in a pionless effective field theory up to NLO. We first use the deuteron binding energy and the ANC to fix the LECs of the contact interactions by solving the lattice form of the Lippmann-Schwinger equation with Lanczos technique. Then we employ Lüscher's finite-volume relation to extract the S-wave ERE parameters $r^{(^3S_1)}$ and $a^{(^3S_1)}$ from the lattice energy eigenvalues corresponding to the different lattice size. The lattice spacing dependence of the ERE parameters is studied in the range $1.4 \le a \le 2.6$ fm. To eliminate the lattice artifacts, an $\mathcal{O}(a^4)$ -improved lattice action is considered. The impact of different powers of the exponential regulator is studied for the lattice spacing a = 1.97 fm, and it is shown that they have an almost similar influence on the extracted ERE parameters. The introduced regulator is applied to different lattice

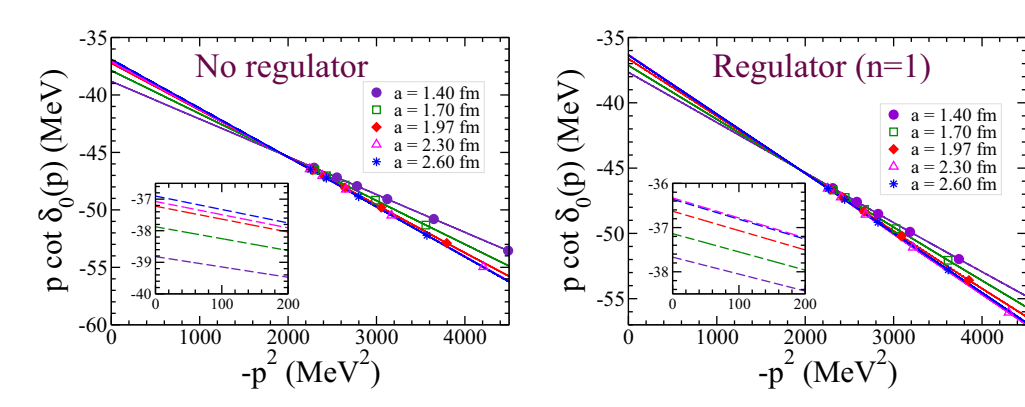


FIG. 4. The NLO EFT results for the effective range function $p \cot \delta_0(p)$ in the 3S_1 neutron-proton channel for different values of lattice spacing parameter a. In the left panel, the results are obtained with bare contact interactions with no regulator, and in the right panel, a regulator with power n = 1 and the parameter b = 0.01 is applied.

TABLE IV. Deuteron binding energy, ANC and the ERE parameters $a^{(3S_1)}$ and $r^{(3S_1)}$ calculated for different lattice spacing parameter a with and without implementing the regularization scheme, suggested in Eqs. (13) and (14). The numbers in parentheses are the uncertainties in the last digits.

a (fm)	C_0^L	$C_2^L \times 10^{-2}$	E ₂ (MeV)	ANC (fm ^{-0.5})	$a^{(^3S_1)}$ (fm)	$r^{(^{3}S_{1})}$ (fm)
			No Res	gulator		
1.4	-2.142950	+4.7378272	-2.224575	0.249422	5.08(1)	1.288(7)
1.7	-1.816890	+3.7820497	-2.224575	0.249424	5.23(3)	1.49(2)
1.97	-1.579070	+3.0453214	-2.224575	0.249425	5.35(3)	1.65(2)
2.3	-1.233188	+1.9176492	-2.224575	0.249423	5.32(5)	1.68(4)
2.6	-0.978510	+1.2371360	-2.224576	0.249426	5.35(5)	1.70(5)
		With Ro	egulator ($n = 1, b = .$	A/a^3 ; $A = 0.07645373$	fm^3)	
1.4	-2.064	+5.1448251	-2.224577	0.246912	5.22(4)	1.47(2)
1.7	-1.79465	+3.9924816	-2.224575	0.249424	5.33(6)	1.60(4)
1.97	-1.59677	+3.2940765	-2.224575	0.249424	5.43(5)	1.74(4)
2.3	-1.323997	+2.3189424	-2.224575	0.249425	5.43(3)	1.81(3)
2.6	-1.02118	+1.3854333	-2.224574	0.249427	5.42(5)	1.79(4)
Experiment	_	_	-2.224575	0.249424	5.424(4)	1.759(5)

TABLE V. Comparison of our ERE parameters in the 3S_1 channel, obtained with and without the application of the regularization scheme, with the results of other groups. The parameters (n, b) indicate the regulator parameters, introduced in Eq. (14). The numbers in parentheses are the uncertainties in the last digits.

Method	а	$a^{(^3S_1)}$ (fm)	$r^{(^3S_1)}$ (fm)
Present (n, b)			
LO (1, 0)	1.97 fm	4.577(7)	0.496(8)
LO (1, 0.01)	1.97 fm	4.652(7)	0.621(7)
LO (2, 0.01)	1.97 fm	4.624(7)	0.580(8)
LO (3, 0.01)	1.97 fm	4.64(1)	0.60(1)
NLO (1, 0)	1.97 fm	5.35(3)	1.65(2)
NLO (1, 0.01)	1.97 fm	5.43(5)	1.74(4)
NLO (2, 0.01)	1.97 fm	5.41(4)	1.73(3)
NLO (3, 0.01)	1.97 fm	5.42(3)	1.76(2)
Borasoy et al. (LO Pionless EFT) [4]	1.97 fm	4.522(1)	0.30(2)
	1.97 fm	4.664(1)	0.53(2)
Rokash et al. (LO Pionless EFT) [16]	2 fm	4.50	0.33
Klein et al. (LO Pionless EFT) [18]	1.97 fm	5.611(1)	2.029(1)
Klein et al. (LO pionfull EFT) [18]	1.97 fm	5.470(1)	1.818(1)
Alarcón et al. (LO pionfull EFT) [20]	1.97 fm	5.46(1)	1.686(1)
Alarcón et al. (NLO pionfull EFT) [20]	1.97 fm	5.31(2)	1.79(3)
Alarcón et al. (N ² LO pionfull EFT) [20]	1.97 fm	5.35(2)	1.82(3)
Experiment		5.424(4)	1.759(5)

spacing, leading to an improvement on the extraction of the ERE parameters, and brings them close to the experimental data for $a \ge 2$ fm.

ACKNOWLEDGMENTS

We thank Koji Harada for sharing their results, which allowed us to validate our codes for the solution of the Lippmann-Schwinger equation for two-nucleon-bound states on a lattice. The work of M.R.H. was supported by the

National Science Foundation under Grant No. NSF-PHY-2000029 with Central State University.

APPENDIX: TWO-NUCLEON ENERGY EIGENVALUES

In Tables VII–XI, we provide our numerical results for the solution of the Lippmann-Schwinger equation, given in Eq. (9), with the LECs given in Table VI, for different values of lattice spacing parameter a and different number of lattice nodes N_s .

TABLE VI. The LECs C_0^L and C_2^L fitted to deuteron binding energy and ANC for different lattice spacing parameter a with and without implementing the regularization scheme, introduced in Eqs. (13) and (14). n indicates the power of the exponential regulator.

a (fm)	C_0^L	$C_2^L \times 10^{-2}$
	No Reş	gulator
1.4	-2.142950	+4.7378272
1.7	-1.816890	+3.7820497
1.97	-1.579070	+3.0453214
2.3	-1.233188	+1.9176492
2.6	-0.978510	+1.2371360
	With Regula	ator $(n=1)$
1.4	-2.064	+5.1448251
1.7	-1.79465	+3.9924816
1.97	-1.59677	+3.2940765
2.3	-1.323997	+2.3189424
2.6	-1.02118	+1.3854333
	With Regula	ator $(n=2)$
1.97	-1.587607	+3.4237993
	With Regula	ntor (n = 3)
1.97	-1.574284	+3.945544

TABLE VII. Deuteron binding energy calculated for different values of N_s with the lattice spacing a = 1.4 fm. The parameters (n, b) indicate the regulator parameters, introduced in Eq. (14).

N_s	NLO $(n = 1, b = 0)$	NLO $(n = 1, b = 2.786215 \times 10^{-2})$
20	-2.224575	-2.224577
18	-2.236165	-2.237620
16	-2.261734	-2.265850
14	-2.318403	-2.327441
12	-2.443624	-2.461672
10	-2.717962	-2.752608
9	-2.960845	-3.008798
8	-3.325327	-3.392493
7	-3.885172	-3.981742
6	-4.781351	-4.926780
5	-6.316952	-6.553276
4	-9.250943	-9.680334

TABLE VIII. The same as Table VII, but for a = 1.7 fm.

N_s	NLO $(n = 1, b = 0)$	NLO $(n = 1, b = 1.556152 \times 10^{-2})$
20	-2.224575	-2.224577
18	-2.227704	-2.228103
16	-2.235686	-2.236853
14	-2.256377	-2.259115
12	-2.310365	-2.316613
10	-2.452207	-2.465131
9	-2.592639	-2.611437
8	-2.818116	-2.845511
7	-3.183195	-3.223659
6	-3.789626	-3.851409
5	-4.852515	-4.953149
4	-6.904684	-7.086130

TABLE IX. The same as Table VII, but for a = 1.97 fm.

	LO					N	LO	
N_s	No Reg.	n = 1	n = 2	n=3	No Reg.	n = 1	n = 2	n=3
20	-2.224575	-2.224573	-2.224576	-2.224575	-2.224575	-2.224575	-2.224574	-2.224575
18	-2.225251	-2.225346	-2.225263	-2.225265	-2.225550	-2.225704	-2.225583	-2.225610
16	-2.227186	-2.227485	-2.227247	-2.227244	-2.228361	-2.228816	-2.228490	-2.228589
14	-2.232922	-2.233633	-2.233106	-2.233127	-2.236632	-2.237740	-2.237041	-2.237354
12	-2.250310	-2.251998	-2.250869	-2.251025	-2.261507	-2.264124	-2.262728	-2.263680
10	-2.304263	-2.308227	-2.305968	-2.306441	-2.337196	-2.343432	-2.340805	-2.343569
9	-2.365196	-2.371330	-2.368068	-2.368943	-2.420902	-2.430523	-2.426944	-2.431602
8	-2.472692	-2.482165	-2.477541	-2.479011	-2.565747	-2.580570	-2.575767	-2.583490
7	-2.661788	-2.676394	-2.669839	-2.672291	-2.815834	-2.838765	-2.832374	-2.845091
6	-2.995661	-3.018378	-3.009063	-3.013079	-3.252139	-3.288325	-3.279835	-3.301075
5	-3.598996	-3.635343	-3.621888	-3.628761	-4.041911	-4.102015	-4.091016	-4.129732
4	-4.755451	-4.817499	-4.797340	-4.811362	-5.592160	-5.701678	-5.683439	-5.743210

TABLE X. The same as Table VII, but for a = 2.3 fm.

N_s	NLO $(n = 1, b = 0)$	NLO $(n = 1, b = 6.283696 \times 10^{-3})$
20	-2.224575	-2.224575
18	-2.224804	-2.224863
16	-2.225572	-2.225748
14	-2.228180	-2.228647
12	-2.237352	-2.238583
10	-2.270483	-2.273990
9	-2.312144	-2.318053
8	-2.391733	-2.401826
7	-2.542779	-2.559982
6	-2.828306	-2.857706
5	-3.375589	-3.427266
4	-4.483011	-4.581039

TABLE XI. The same as Table VII, but for a = 2.6 fm.

N_s	NLO $(n = 1, b = 0)$	NLO $(n = 1, b = 4.3498936 \times 10^{-3})$
20	-2.224576	-2.224574
18	-2.224638	-2.224659
16	-2.224869	-2.224938
14	-2.225771	-2.225941
12	-2.229746	-2.229861
10	-2.244550	-2.245892
9	-2.265714	-2.268085
8	-2.309831	-2.314116
7	-2.401551	-2.409350
6	-2.590731	-2.604906
5	-2.979936	-3.005941
4	-3.802672	-3.852706

- [1] T. A. Lähde and U.-G. Meißner, *Nuclear Lattice Effective Field Theory: An Introduction* (Springer, Berlin, 2019), Vol. 957.
- [2] H.-M. Müller, S. E. Koonin, R. Seki, and U. van Kolck, Nuclear matter on a lattice, Phys. Rev. C 61, 044320 (2000).
- [3] B.-N. Lu, N. Li, S. Elhatisari, D. Lee, E. Epelbaum, and U.-G. Meißner, Essential elements for nuclear binding, Phys. Lett. B 797, 134863 (2019).
- [4] B. Borasoy, E. Epelbaum, H. Krebs, D. Lee, and U.-G. Meißner, Lattice simulations for light nuclei: Chiral effective field theory at leading order, Eur. Phys. J. A 31, 105 (2007).
- [5] B. Borasoy, E. Epelbaum, H. Krebs, D. Lee, and U.-G. Meißner, Chiral effective field theory on the lattice at next-to-leading order, Eur. Phys. J. A 35, 343 (2008).
- [6] D. Lee, Lattice simulations for few-and many-body systems, Prog. Part. Nucl. Phys. 63, 117 (2009).
- [7] E. Epelbaum, H.-W. Hammer, and Ulf.-G. Meißner, Modern theory of nuclear forces, Rev. Mod. Phys. **81**, 1773 (2009).
- [8] R. Machleidt and D. R. Entem, Chiral effective field theory and nuclear forces, Phys. Rep. **503**, 1 (2011).
- [9] M. Pine, D. Lee, and G. Rupak, Adiabatic projection method for scattering and reactions on the lattice, Eur. Phys. J. A 49, 151 (2013).
- [10] S. Elhatisari, D. Lee, U.-G. Meißner, and G. Rupak, Nucleon-deuteron scattering using the adiabatic projection method, Eur. Phys. J. A **52**, 174 (2016).
- [11] K. Harada, S. Sasabe, and M. Yahiro, Numerical study of renormalization group flows of nuclear effective field theory without pions on a lattice, Phys. Rev. C 94, 024004 (2016).
- [12] M. Luscher, Volume dependence of the energy spectrum in massive quantum field theories. 2. Scattering states, Commun. Math. Phys. 105, 153 (1986).
- [13] S. R. Beane, P. F. Bedaque, A. Parreno, and M. J. Savage, Two nucleons on a lattice, Phys. Lett. B 585, 106 (2004).

- [14] S. Bour, S. König, D. Lee, H.-W. Hammer, and Ulf.-G. Meißner, Topological phases for bound states moving in a finite volume, Phys. Rev. D 84, 091503(R) (2011).
- [15] S. Bour, H.-W. Hammer, D. Lee, and Ulf.-G. Meißner, Benchmark calculations for elastic fermion-dimer scattering, Phys. Rev. C 86, 034003 (2012).
- [16] A. Rokash, E. Epelbaum, H. Krebs, D. Lee, and U.-G. Meißner, Finite volume effects in low-energy neutron-deuteron scattering, J. Phys. G: Nucl. Part. Phys. 41, 015105 (2013).
- [17] N. Klein, D. Lee, and U.-G. Meißner, Lattice improvement in lattice effective field theory, Eur. Phys. J. A 54, 1 (2018).
- [18] N. Klein, D. Lee, W. Liu, and U.-G. Meißner, Regularization methods for nuclear lattice effective field theory, Phys. Lett. B 747, 511 (2015).
- [19] N. Klein, S. Elhatisari, T. A. Lähde, D. Lee, and U.-G. Meißner, The Tjon band in nuclear lattice effective field theory, Eur. Phys. J. A 54, 121 (2018).
- [20] J. M. Alarcón, D. Du, N. Klein, T. A. Lähde, D. Lee, N. Li, B.-N. Lu, T. Luu, and U.-G. Meißner, Neutron-proton scattering at next-to-next-to-leading order in nuclear lattice effective field theory, Eur. Phys. J. A 53, 83 (2017).
- [21] M. Eliyahu, B. Bazak, and N. Barnea, Extrapolating lattice QCD results using effective field theory, arXiv:1912.07017.
- [22] M. R. Hadizadeh, M. T. Yamashita, L. Tomio, A. Delfino, and T. Frederico, Binding and structure of tetramers in the scaling limit, Phys. Rev. A 85, 023610 (2012).
- [23] D. R. Phillips, G. Rupak, and M. J. Savage, Improving the convergence of nn effective field theory, Phys. Lett. B 473, 209 (2000).
- [24] E. Epelbaum, W. Glöckle, and U.-G. Meißner, Nuclear forces from chiral Lagrangians using the method of unitary transformation II: The two-nucleon system, Nucl. Phys. A 671, 295 (2000).